

RESEARCH ARTICLE

Ribitol dose-dependently enhances matriglycan expression and improves muscle function with prolonged life span in limb girdle muscular dystrophy 2I mouse model

Bo Wu*, Morgan Drains, Sapana N. Shah, Pei Juan Lu, Victoria Leroy, Jessalyn Killilee, Raegan Rawls , Jason D. Tucker , Anthony Blaeser, Qi Long Lu *

McCull-Lockwood Laboratory for Muscular Dystrophy Research, Atrium Health Musculoskeletal Institute, Carolinas Medical Center, Charlotte, North Carolina, United States of America

* Bo.Wu@atriumhealth.org (BW); Qi.Lu@atriumhealth.org (QLL)



OPEN ACCESS

Citation: Wu B, Drains M, Shah SN, Lu PJ, Leroy V, Killilee J, et al. (2022) Ribitol dose-dependently enhances matriglycan expression and improves muscle function with prolonged life span in limb girdle muscular dystrophy 2I mouse model. PLoS ONE 17(12): e0278482. <https://doi.org/10.1371/journal.pone.0278482>

Editor: Girish C. Melkani, UAB School of Medicine, UNITED STATES

Received: April 8, 2022

Accepted: November 16, 2022

Published: December 1, 2022

Copyright: © 2022 Wu et al. This is an open access article distributed under the terms of the [Creative Commons Attribution License](https://creativecommons.org/licenses/by/4.0/), which permits unrestricted use, distribution, and reproduction in any medium, provided the original author and source are credited.

Data Availability Statement: All relevant data are within the manuscript and its [Supporting information](#) files.

Funding: This work was supported by the Carolinas Muscular Dystrophy Research Endowment through the Atrium Health Foundation at Charlotte, NC. The funders had no role in study design, data collection and analysis, decision to publish, or preparation of the manuscript.

Abstract

Limb Girdle Muscular Dystrophy 2I (LGMDR9) is one of the most common LGMD characterized by defects in glycosylation of α -dystroglycan (matriglycan) resulting from mutations of Fukutin-related protein (FKRP). There is no effective therapy currently available. We recently demonstrated that ribitol supplement increases levels of matriglycan in cells *in vitro* and in FKRP-P448L (*P448L*) mutant mouse model through drinking water administration. To be clinically relevant, we have now conducted a dose-escalating efficacy study by gavage in *P448L* mutant mice. Six months of ribitol treatment daily significantly rescued functions of skeletal, respiratory, and cardiac muscles dose-dependently. This was associated with a dose dependent increase in matriglycan and improvement in muscle pathology with reductions in muscle degeneration, inflammatory infiltration and fibrosis. Importantly, ribitol significantly increased life span and muscle functions of the female animals receiving treatment from 10 months of age. The only observed side effect was gastrointestinal tract bloating with loose stool and this effect is also dose dependent. The results validate the mechanism that ribitol as a pre-substrate of glycosyltransferase is able to compensate for the decreased function of mutant FKRP with restoration of matriglycan expression and provide a guidance for future clinical trial design.

Introduction

Mutations in Fukutin-related protein (FKRP) cause muscular dystrophy with wide range of disease phenotypes from mild limb girdle muscular dystrophy 2I (LGMDR9) to severe congenital muscular dystrophy (CMD), Walker-Warburg syndrome (WWS), and muscle-eye-brain (MEB) disease [1–3]. The common features of the diseases are progressive muscle degeneration and loss of function including both skeletal and cardiac muscles. Consequently, patients gradually lose mobility with impairment, and ultimately failure of respiratory and cardiac functions [4, 5]. The severe CMD, WWS and MEB have defects in central nerve and optical

Competing interests: I have read the journal's policy and the authors of this manuscript have the following competing interests: Q.L.L. is the consultant of ML Bio Solution which is conducting clinical trial with ribitol for LGMD2I.

systems with developmental delay and cognitive impairment [1, 2]. Currently no treatment is available although several experimental therapies are being tested pre-clinically [6, 7].

The biochemical alteration underlining muscle weakness of the diseases is hypoglycosylation of alpha-dystroglycan (α -DG). Alpha-DG is a peripheral membrane protein glycosylated with O-linked glycans capable of binding to laminin as well as other extracellular matrix (ECM) proteins, including agrin, perlecan, neurexin and pikachurin [8–13]. The interaction of α -DG with ECM proteins is critical for maintaining muscle integrity. The structure of the laminin-binding O-mannosylated glycan (matriglycan) has recently been delineated with individual enzymes identified [14–16]. FKRPs function as glycosyltransferases using CDP-ribitol as its substrate to add ribitol-5-phosphate (R-5-P) to the backbone of the O-mannosylated glycan. This permits further addition of laminin-binding GlcA-Xyl dimer repeats. Recent studies also identified isoprenoid synthase domain containing (ISPD) as a cytidyltransferase producing CDP-ribitol [16, 17]. Gerin et al. further demonstrated that ribitol treatment of ISPD-deficient cells leads to an increase of CDP-ribitol levels and partially corrects the defect in matriglycan synthesis [16]. The authors also reported that supply of ribitol can increase matriglycan in wild-type cells. We reported earlier that FKRPs mutations such as P448L associated with severe CMD phenotype retain partial biological function and are capable of maintaining up to near normal levels of matriglycan in new-born and regenerating fibers [18, 19]. We recently reported that ribitol is able to partially restore matriglycan in the dystroglycanopathy model with mutations in FKRPs gene [20–22]. Administration of ribitol within drinking water increases levels of R-5-P and CDP-ribitol and restores therapeutic levels of matriglycan in skeletal and cardiac muscles.

However, administration of ribitol by drinking water *ad libitum* as a treatment for FKRPs-related muscular dystrophies is not clinically applicable. Furthermore, effective dose range of ribitol and treatment regime need to be established for clinical trials. To answer these questions, we have conducted a dose range study with ribitol delivered through daily gavage to the FKRPs-P448L mutant mice. Efficacy of treatment was examined in two age groups, representing the early and later stages in disease progression. Ribitol treatment enhances levels of matriglycan significantly in both cardiac and skeletal muscles with improved pathology and muscle functions. Treatment given at a later stage of the disease is able to prolong the life span. These results, together with the fact that ribitol is a natural metabolite without significant side effect at high doses, warrants further development by clinical trials as a novel therapy to FKRPs-related muscular dystrophy.

Materials and method

Animal care

All animal studies were approved by the Institutional Animal Care and Use Committee (IACUC) of Carolinas Medical Center, Atrium Health. All mice were housed in the vivarium of Carolinas Medical Center following animal care guidelines of the institute. Animals were ear tagged prior to group assignment. Food and water were available *ad libitum* during all phase of the study. Body weight was measured daily for accurate gavage and minor mouse condition.

Mouse model and experimental procedure

FKRPs-P448L (P448L) mutant mice (C57BL/6N background) containing a homozygous missense mutation (*c.1343C>T*, p.Pro448Leu) were generated by the McColl-Lockwood Laboratory for Muscular Dystrophy Research [21, 22]. C57BL/6 (wild-type/C57) mice were purchased from Jackson Laboratory. Ribitol was purchased from Sigma (A5502 Adonitol, $\geq 98\%$, Sigma,

St. Louis) and dissolved in saline to desired concentrations as 100ul/10g mouse body weight. Three week and 10 month old *P448L* mice were treated with ribitol by gavage with the following doses and regimes: 0.5g/kg, 2g/kg, 5g/kg and 10g/kg body weight once a day. Additionally, 10g/kg daily dose was also administrated as 5g/kg twice a day and 3.3g/kg three times a day for comparison with single dose treatment. Twenty mice (with more than 8 mice for each sex) were randomly assigned to either treatment or control groups. Age-matched *P448L* and wild-type *C57BL/6* mice were gavaged with the same volume of saline as controls. Regular muscle function tests were performed, and the animals were euthanized by cervical spine dislocation under isoflurane anesthesia after 6 months (for the groups starting 3 weeks of age) or longer (for the groups starting 10 months of age) of treatment and tissues including heart, diaphragm, TA, quadriceps, liver, spleen and kidney were collected for analyses (S1 Fig in [S1 File](#)).

Immunohistochemical and western blot analysis

Tissues were dissected and snap-frozen in dry-ice-chilled-2-methylbutane. For immunohistochemical detection of matriglycan, muscle cross sections of 6 μm of thickness were prepared from treated and saline control mice. Slides were first fixed in ice cold Ethanol:Acetic acid (1:1) for 1 min, blocked with 10% normal goat serum (NGS) in 1xTris-buffer saline (TBS) for 30 min at room temperature, and incubated overnight at 4°C with primary mouse monoclonal antibody IIH6C4 (EMD Millipore) (1:500) against matriglycan on α -DG. Negative controls received 10% normal goat serum in 1xTBS without primary antibody. Sections were washed and incubated with secondary AlexaFluor 488 or 594 goat anti-mouse IgM (Invitrogen) (1:500) at room temperature for 2 hr. Sections were then washed and finally mounted with fluorescence mounting medium (Dako) containing 1x DAPI (4',6'-diamidino -2-phenylindole) for nuclear staining. Immunofluorescence was visualized using an Olympus BX51/BX52 fluorescence microscope (Opelco) and images were captured using the Olympus DP70 digital camera system (Opelco). Slides were examined in a blind manner by the investigators.

For western blot analysis, sections cut from tissues were homogenized in extraction buffer (50 mM Tris-HCl pH 8.0, 150 mM NaCl, and 1% Triton X-100), supplemented with 1x protease inhibitor cocktail (Sigma-Aldrich). Protein concentration was quantified by Bradford assay (Bio-Rad DC protein assay). Eighty μg of protein was loaded on an 4–15% Bio-Rad Mini-PROTEAN TGX gel (Bio-Rad) and immunoblotted. Total protein loaded from *C57* mice was half of the amount loaded for the *P448L* mice. Nitrocellulose membranes (Bio-Rad) were blocked with 5% milk in 1xPBS for 2 hr at room temperature and then incubated with the following primary antibodies overnight at 4°C: IIH6C4 (1:2000), and α -actin (Sigma) (1:1000). Horseradish peroxidase (HRP)-conjugated secondary antibodies were incubated for 2 hr at room temperature. All blots were developed by electrochemiluminescence immunodetection (PerkinElmer). ImageJ software was used for IIH6C4 band quantification from western blot.

Histopathological and morphometric analysis

Sections of 6 μm of thickness were processed for hematoxylin and eosin (H&E) and Masson's Trichrome staining following standard procedures. Muscle cross-sectional fiber equivalent diameter were determined from tibialis anterior (TA) and quadriceps stained with H&E using MetaMorph v7.7 Software (Molecular Devices). Percentage of centrally nucleated myofibers were manually quantified from the same tissue sections stained with H&E. Fibrotic area represented by blue staining in the Masson's Trichrome stained sections was quantified from heart, diaphragm, TA and quadriceps using ImageJ software. For all the morphometric analyses, a total of 500 fibers from five representative 20X magnification images per each muscle per animal were used.

Metabolite extraction from muscle tissues and LC/MS-MS analysis

Ribitol was purchased from Sigma (A5502). R-5-P and CDP-ribitol were synthesized by Z Biotech (Aurora, CO). Muscle tissues were collected, and blinded samples were subjected to the following procedure. Thirty to 80 μg of frozen tissue samples was homogenized with 400 μl of MeOH:Acetonitrile (ACN) (1:1) and then centrifugated for 5 min at 10,000 rpm. The supernatants were removed, transferred to individual wells of 96-well plate, and analyzed by LC/MS-MS. An Applied Biosystems Sciex 4000 (Applied Biosystems; Foster City, CA) equipped with a Shimadzu HPLC (Shimadzu Scientific Instruments, Inc.: Columbia, MD) and Leap auto-sampler (LEAP Technologies; Carrboro, NC) were used to detect ribitol, R-5-P and CDP-ribitol from tissue samples and synthetic compounds. The metabolites were separated on a silica gel column (Hypersil Silica 250 x 4.6 mm, 5 micron particle size) using solvent A: water, 10mM NH_4OAc , 0.1% formic acid and solvent B: MeOH:ACN (1:1). The following gradient was used: 0–12 min, 5% buffer B; 13–14 min, 95% buffer B, 15–17 min, 5% buffer B. Under these conditions, ribitol, R-5-P and CDP-ribitol eluted at 8.3 min, 7.5 min and 8.9 min, respectively. The metabolites were analyzed using electrospray ionization mass spectrometry operated in positive ion mode, ESI+. Compounds concentration in tissue samples were determined based on standard curves prepared by serial dilutions (200–0.01 μM) of each of the compound in MeOH:ACN (1:1).

Grip strength and treadmill test

Grip strength was assessed using a grip strength meter consisting of horizontal forelimb mesh and an angled hind limb mesh (Columbus Instruments, Columbus, OH). Five successful forelimb and hind limb strength measurements within 2 minutes were recorded, and data were normalized to body weight (BW). Treadmill test was performed on LE8700 treadmill (Panlab/Harvard Apparatus, Barcelona, Spain) supplied with shock grids mounted at the back of the treadmill, which delivered a 0.2 mA current to provide motivation for exercise. The end points were mice exhaustion, as demonstrated by the animal remaining on the shock grid for 10 consecutive seconds without getting off or 50% on/off within 1-minute period (for details, see reference 6).

Whole body plethysmography

Respiratory functional analysis in conscious, freely moving mice were measured using a whole-body plethysmography technique. The plethysmograph apparatus (Emka Technologies, Falls Church, VA) was connected to a ventilation pump for maintaining a constant air flow, a differential pressure transducer, a usbAMP signal amplifier, and a computer running EMKA iox2 software with the respiratory flow analyzer module, which was used to detect pressure changes due to breathing and recording the transducer signal. After calibration, mice were placed inside the “free moving” plethysmograph chamber and allowed to acclimate for 5 min to minimize any effects of stress related changes in ventilation. Resting ventilation was measured for a duration of 15 min after the acclimation period. Body temperatures of mice were assumed to be 37°C and to remain constant during the ventilation protocol.

Echocardiogram

Echocardiogram was performed using the BioscanSonixTablet Ultrasound System (Analogic Ultrasound, Peabody, MA). Detailed method was published by Blaeser et al. [23].

Statistical analysis

All the results were expressed as means + SEM. One-Way ANOVA was used for comparing treatments with control group. Differences were considered statistically significant at $p \leq 0.05$ (*).

Results

Assessment for maximum tolerable daily dose of ribitol in *P448L* mice

Our earlier study of ribitol treatment by drinking water in *P448L* mutant mice suggests that up to 10% ribitol ad libitum was safe [20]. By measuring the amount of water consumed daily (about 1 ml water consumed by a mouse of 10g body weight), 10% ribitol in drinking water delivers roughly 10g ribitol per kg body weight daily. We therefore first examined the effect of ribitol by gavage with 10g/kg once a day for 1 month in *P448L* mutant mice aged 4–6 weeks old. All 10 mice survived with the treatment although a majority displayed clearly visible signs of diarrhea and gastrointestinal (GI) bloating, which was confirmed at autopsy (S2A Fig in [S1 File](#)). No significant difference was observed in body weight, or in serum markers for liver and kidney function between ribitol treated and saline-treated control mice (S2B Fig in [S1 File](#)). Immunohistochemistry showed an enhanced expression of matriglycan in all three types of muscles, heart, diaphragm, and TA (S2C Fig in [S1 File](#)). We also measured the blood glucose levels within 48 hours after single dose gavage of 10g ribitol/kg body weight. No significant difference was observed. (S2D Fig in [S1 File](#)). We ultimately decided to use the maximum daily 10g/kg dose, as further increase in dosage to 20g/kg resulted in severe GI effects and morbidity.

Early treatment of ribitol dose-dependently improved matriglycan levels in muscles of *P448L* mutant mice

To determine the effective dose range, we examined 4 daily doses of ribitol by gavage, from 0.5g/kg, 2g/kg, 5g/kg to 10g/kg body weight starting at 3 weeks of age in the *P448L* mutant mice. The lower 3 doses were delivered once a day, whereas the 10g/kg was delivered in 3 different regimes, once daily, 5g/kg twice a day and 3.3g/kg three times a day for comparison. Six-month treatment dose-dependently and significantly enhanced the levels of matriglycan expression as illustrated in [Fig 1](#). Treatment with 0.5g/kg did not produce clearly identifiable enhancement in matriglycan levels examined by immunohistochemistry with I1H6 antibody although weak membrane signal was present. However, clearly definable membrane staining for matriglycan was detected with the 2g/kg ribitol treatment in all three types of muscles ([Fig 1A & 1B](#)). Noticeably, the weak membrane signal in the majority of muscle fibers was rather homogenous in intensity within all examined muscles. Signal intensity for matriglycan was further enhanced with 5g/kg ribitol and reached the highest levels with 10g/kg ribitol, but the difference between the 2 highest dose groups was limited. No clear difference was observed between the 3 different regimes of 10g/kg ribitol. Interestingly, more than 90% of muscle fibers in all treated groups were stained weakly to clearly positive from lower dose to higher dose respectively ([Fig 1A](#)). The dose dependent, but not regime-related matriglycan enhancement was confirmed by western blot measurement ([Fig 1B and 1C](#)). Also noticeable was consistent high levels of matriglycan in the cardiac muscle with 5g and 10g/kg treatments ([Fig 1C](#)).

Ribitol treatment for 6 months improves muscle pathology and reduced serum MCK levels

Enhanced expression of matriglycan after ribitol treatment was associated with a dose-dependent improvement in muscle pathology. As illustrated in [Fig 2](#), untreated *P448L* mutant TA

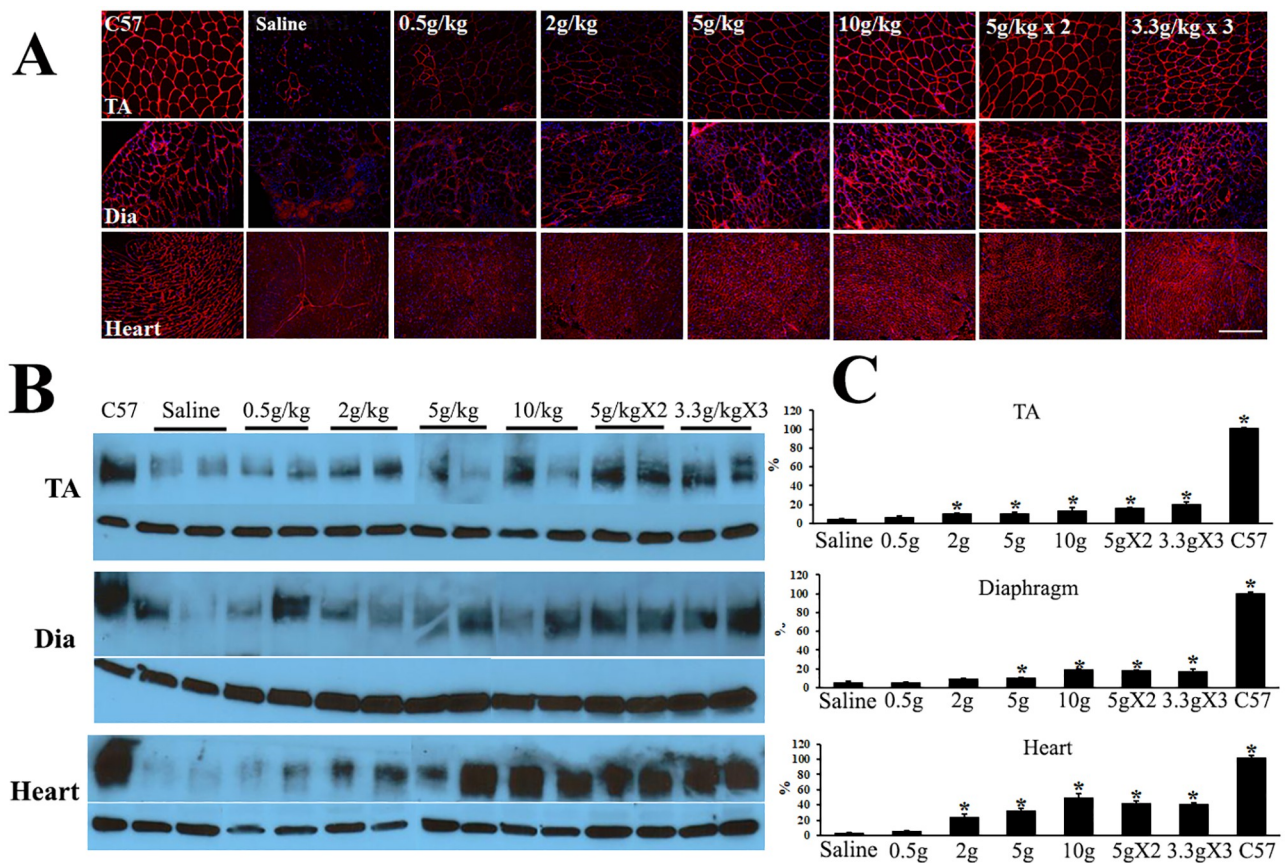


Fig 1. Six-month ribitol treatment enhances matriglycan expression dose-dependently in *P448L FKRP* mutant mice. (A) IHC immunohistochemistry for the detection of matriglycan. Saline treated as control. TA, Tibialis anterior. Dia, diaphragm. (B) Western blots for the detection of matriglycan with IHC6 antibody (with broad bands). Two samples for each dose are shown. The lower panels are α -actin as loading control. (C) measurement of the matriglycan bands by NIH ImageJ with C57 as 100% control. Saline, saline treated; 0.5g, 0.5g/kg; 5gX2, 5g/kg twice a day; 3gX3, 3g/Kg 3 times a day. * $P < 0.05$ $n = 3$ compared to the saline control group. Scale bar = 150 μ M.

<https://doi.org/10.1371/journal.pone.0278482.g001>

and diaphragm muscles showed large foci of fiber degeneration, heavy inflammatory infiltration, and high percentage of centrally nucleated fibers (CNF) with large variation in fiber size. Treatment with 0.5g/kg reduced the area with heavy infiltration although foci of small-sized regenerating fibers remained clearly observed (Fig 2A). Increasing dose of ribitol from 2g/kg to 10g/kg reduced the area of small regenerating fibers and infiltration. This was supported by a more homogeneous fiber size distribution, with less percentage of large fibers as described in Fig 2B. Furthermore, percentage of CNF in the treated skeletal muscles decreased dose-dependently (Fig 2C and 2D). Histological improvement was supported by the similarly dose-dependent decrease in serum creatine kinase levels (Fig 2E). Histological change was not clearly detected in cardiac muscle with ribitol treatment (S3 Fig in S1 File).

Improvement in muscle pathology was most visibly demonstrated by Masson Trichrome staining for the measurement of fibrotic areas within the diseased muscles. A dose-dependent and statistically significant decrease in fibrotic areas was detected in all three muscles, TA, diaphragm, and heart when compared to the corresponding saline-treated control muscles (Fig 3). However, no difference was detected within 3 delivery regimes of the same 10g/kg daily dose.

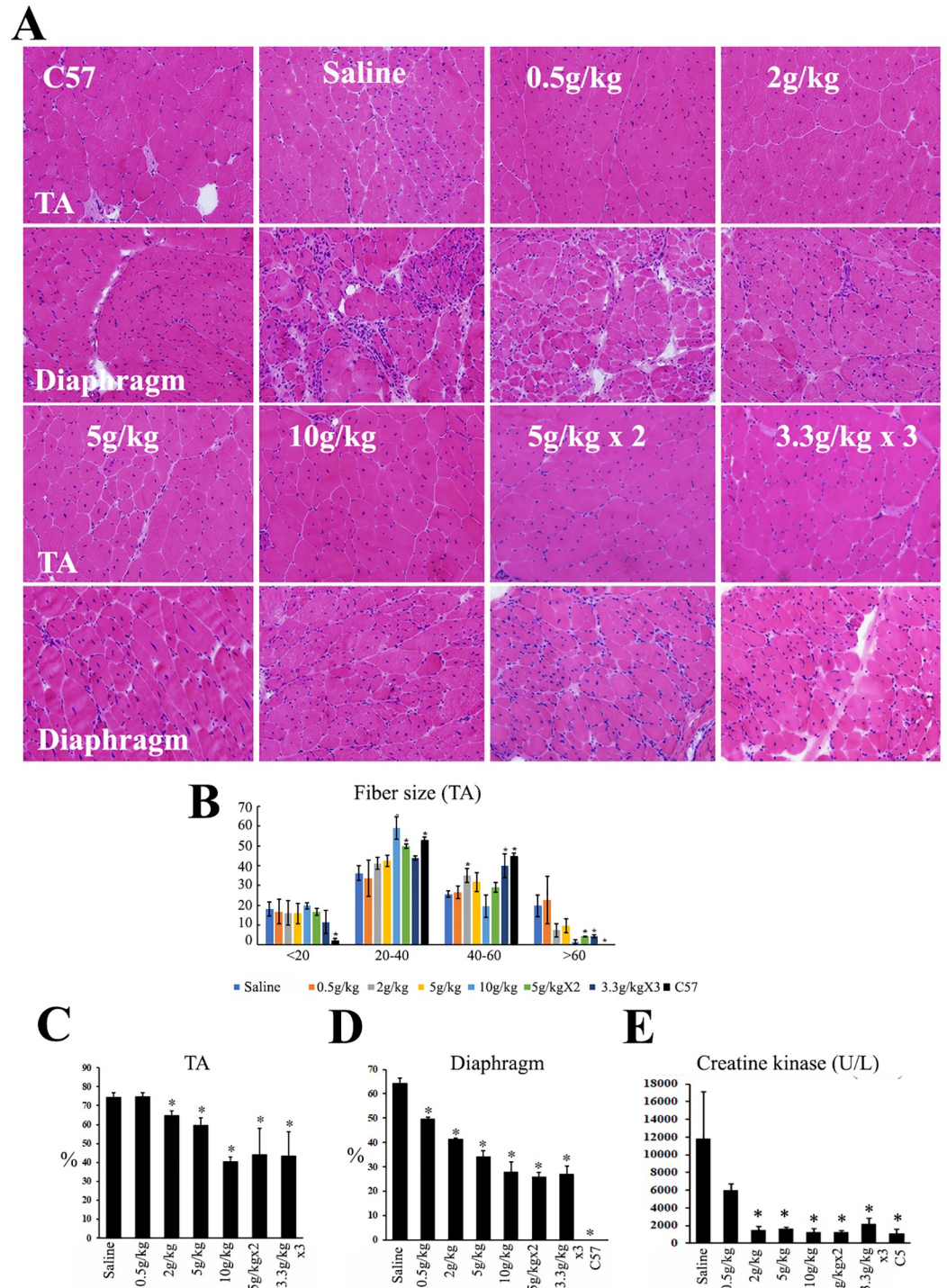


Fig 2. Dose-dependent improvement in muscle pathology of P448L mutant mice after ribitol treatment. (A) H&E staining of skeletal muscles, Tibialis anterior (TA) and diaphragm. (B) Fiber size (μm in diameter) distribution as a percent of the total fibers. $n = 5$. (C) and (D) Percentage of centrally nucleated fibers in TA and diaphragm. $n = 5$. (E) Serum levels of creatine kinase. $n = 10$. * $P < 0.05$ when compared with saline-treated control.

<https://doi.org/10.1371/journal.pone.0278482.g002>

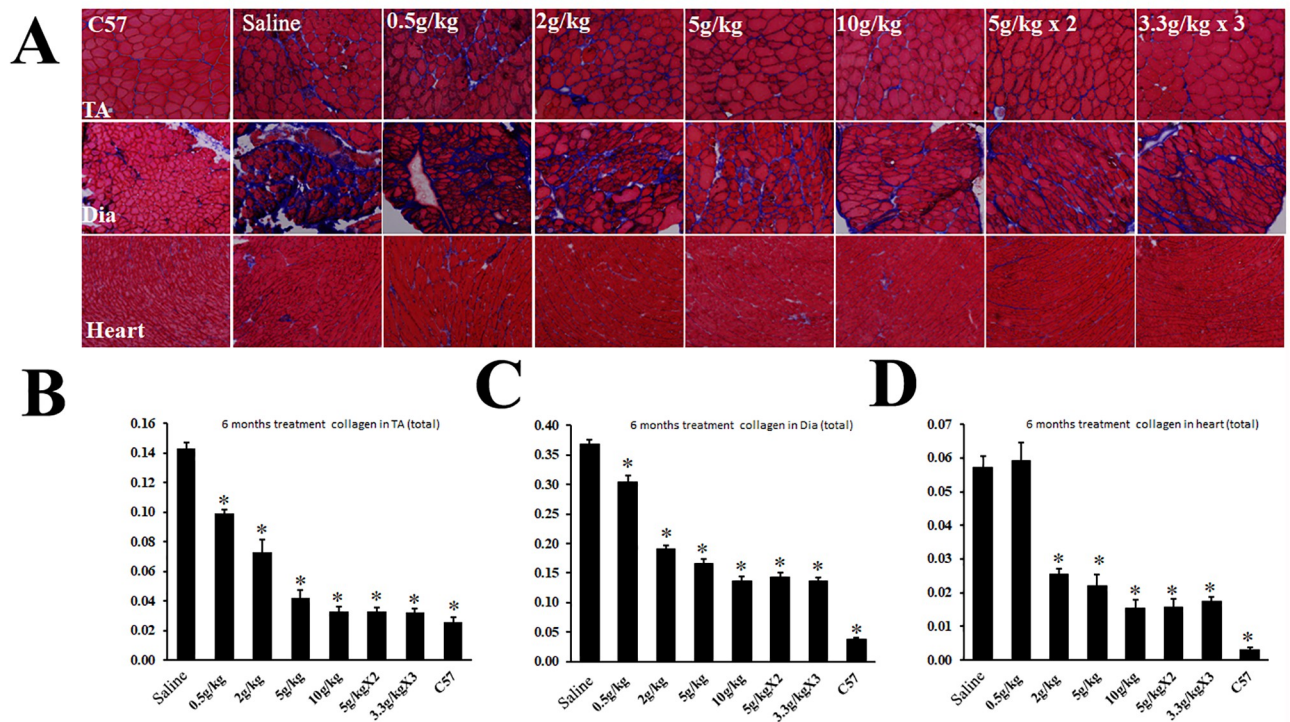


Fig 3. Masson Trichrome staining for the measurement of fibrotic areas in the 6-month ribitol-treated *P448L* mutant mice. (A) Microscopic image of the staining with blue color representing fibrotic areas and red color the remaining muscle fibers. (B-D) Measurement of fibrotic areas with NIH ImageJ. Y axis represents percentage of fibrotic area within the total section area (1 equals to 100% of area measured). * $P < 0.05$ $n = 5$ when compared with saline-treated control.

<https://doi.org/10.1371/journal.pone.0278482.g003>

Effects of six-month ribitol treatments on functions of skeletal and cardiac muscles

Six-month treatment of ribitol did not affect the body weight significantly although 0.5g/kg group showed slightly higher mean body weight than all other groups. Treadmill exhaustion tests showed no significant difference between saline group and 0.5g/kg ribitol group. In contrast, except for the 10g/kg single delivery group, all other 4 groups with 2g/kg and higher doses of ribitol improved running distance and time and the 3.3g/kg 3 times delivery group showed statistical significance (Fig 4A–4C). The decrease in treadmill performance in the 10g/kg single delivery group was associated with strong GI side effect including chronic diarrhea (loose stool) which likely affects exercise performance, especially in endurance. Similarly, grip force strength was also significantly improved for the groups of 5g/kg twice a day and 3.3g/kg 3 times a day regime (Fig 4D and 4E). For respiratory function, significant improvement was also observed in Peak Inspiratory Flow (PIF) and Expiratory Flow (PEF) for 5g/kg or higher dose groups (Fig 4F and 4G; S4 Fig in S1 File). Importantly and consistent with decrease in fibrosis, improvement in cardiac function was indicated by reduction in heart rate and myocardium thickness with 4 groups of 2g/kg or higher dose treatment (Fig 4H and 4I; S5 Fig in S1 File).

Side effects of ribitol treatment

Ribitol treatment was well tolerated with body weight remaining consistent with all groups of mice during the treatment period. H&E staining showed that kidney, liver, and spleen from all

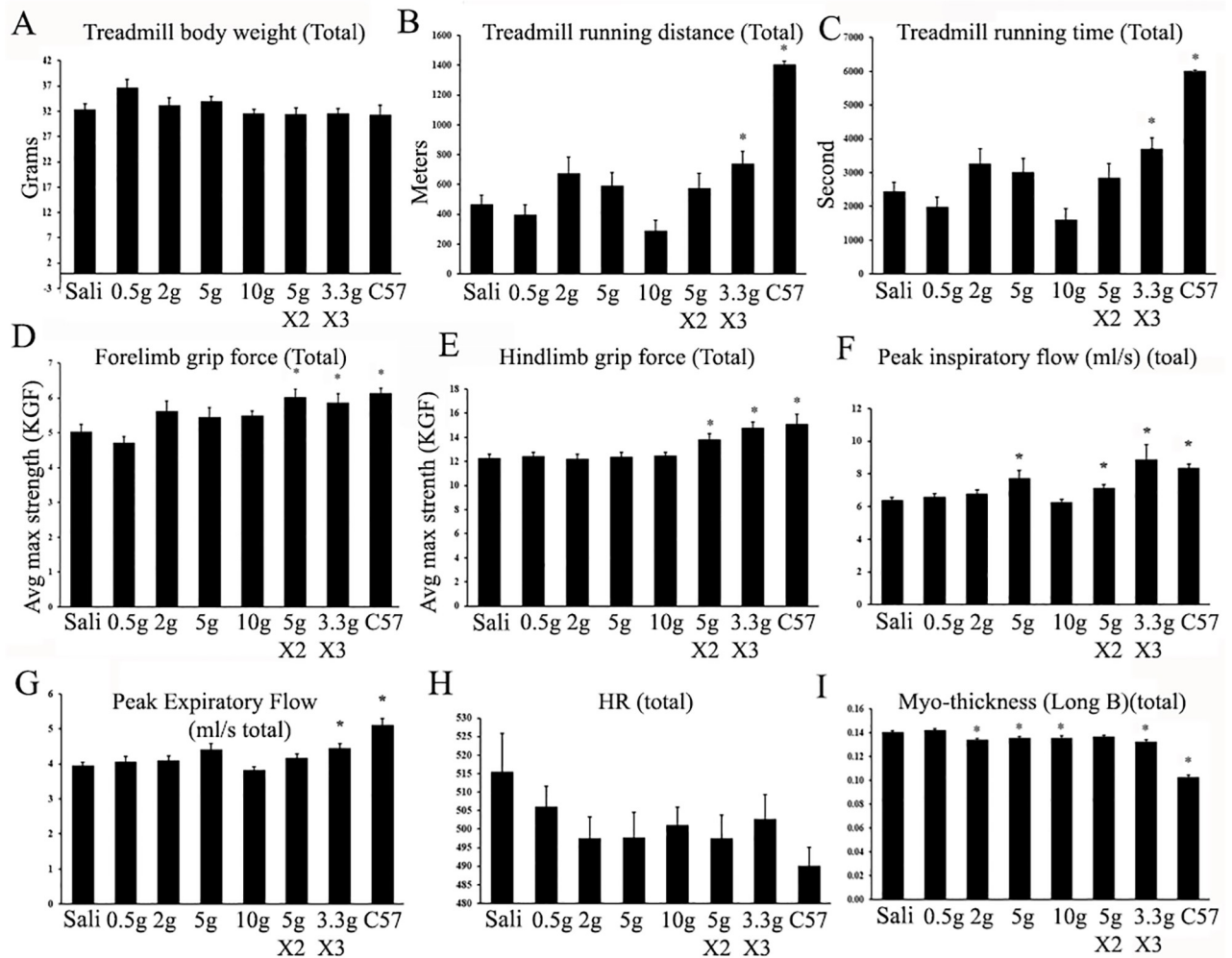


Fig 4. Effect of 6 month ribitol treatment on muscle functions. Skeletal muscle functions were measured by treadmill (A-C) and grip force (D-E). Respiratory and cardiac functions were measured by plethysmography (F-G) and echocardiography (H-I). Sali, saline-treated; 0.5g, 0.5g/kg; 5gX2, 5k/kg twice a day; 3gX3, 3g/Kg 3 times a day. * $p < 0.05$ $n = 20$ when compared with saline-treated *P448L* control.

<https://doi.org/10.1371/journal.pone.0278482.g004>

treatment groups were histologically normal (S6 Fig in [S1 File](#)). The only obvious side effect was the persistent GI bloating and diarrhea with severity being dose dependent. The most severe GI symptom was seen with 10g/kg single gavage whereas the same daily dose administered across 2 and 3 times a day showed milder reaction. Symptoms of GI reaction almost disappeared 48 hours after the last treatment (S6 Fig in [S1 File](#)). Measurement of serum markers for liver and kidney showed no difference between treated and saline control mice (S7 Fig in [S1 File](#)). Interestingly, levels of LDL, ALT, total bilirubin and creatinine were reduced towards normal levels in the groups treated with ribitol.

Detection of ribitol-phosphate and CDP-ribitol in serum and muscles of *P448L* mice after 6 months ribitol treatment

Our early study showed that levels of ribitol, R-5-P and CDP-ribitol in muscles of *P448L* mice increased after 5% ribitol treatment in drinking water [20]. To assess the dosing effect on these metabolites, we measured levels of the 3 metabolites in skeletal, cardiac muscle and serum 24

hours after the last gavage of ribitol. Levels of ribitol in serum was clearly dose dependent whereas both R-5-P and CDP-ribitol were only detected in the highest dose group (S8 Fig in S1 File). Similarly, levels of the three metabolites increased dose dependently in both cardiac and skeletal muscles, but levels of CDP-ribitol appeared to plateau at about 5g/kg daily dose in both muscles (Fig 5A and S8 Fig in S1 File).

Ribitol treatment starting at 10 months of age dose-dependently improves muscle function

To assess the effect of ribitol on later stage LGMDR9, we treated *P448L* mutant mice starting from 10 months of age when significant fibrosis, especially in the diaphragm, and functional defects of skeletal muscles have progressed to an advanced stage. Importantly, our early follow-up of *P448L* mutant mice showed that almost all female mice died within 81 weeks of age [23]. We therefore extended the treatment and monitored the mice until they either manifested humane endpoint criteria (i.e., severe weight loss, deteriorating body condition, or inability to rise/ambulate) or reached a predetermined terminal endpoint of 2 years of age. To make relatively meaningful assessment of ribitol treatment on muscle function of the older mice, we performed skeletal, respiratory and cardiac function evaluation 6 months after initiation of the treatment when no mouse had expired in any experimental group.

Six-month ribitol treatment decreased the levels of creatine kinase and ALT in all dose groups with ribitol treatment (Fig 5B). The treatment did not change body weight significantly

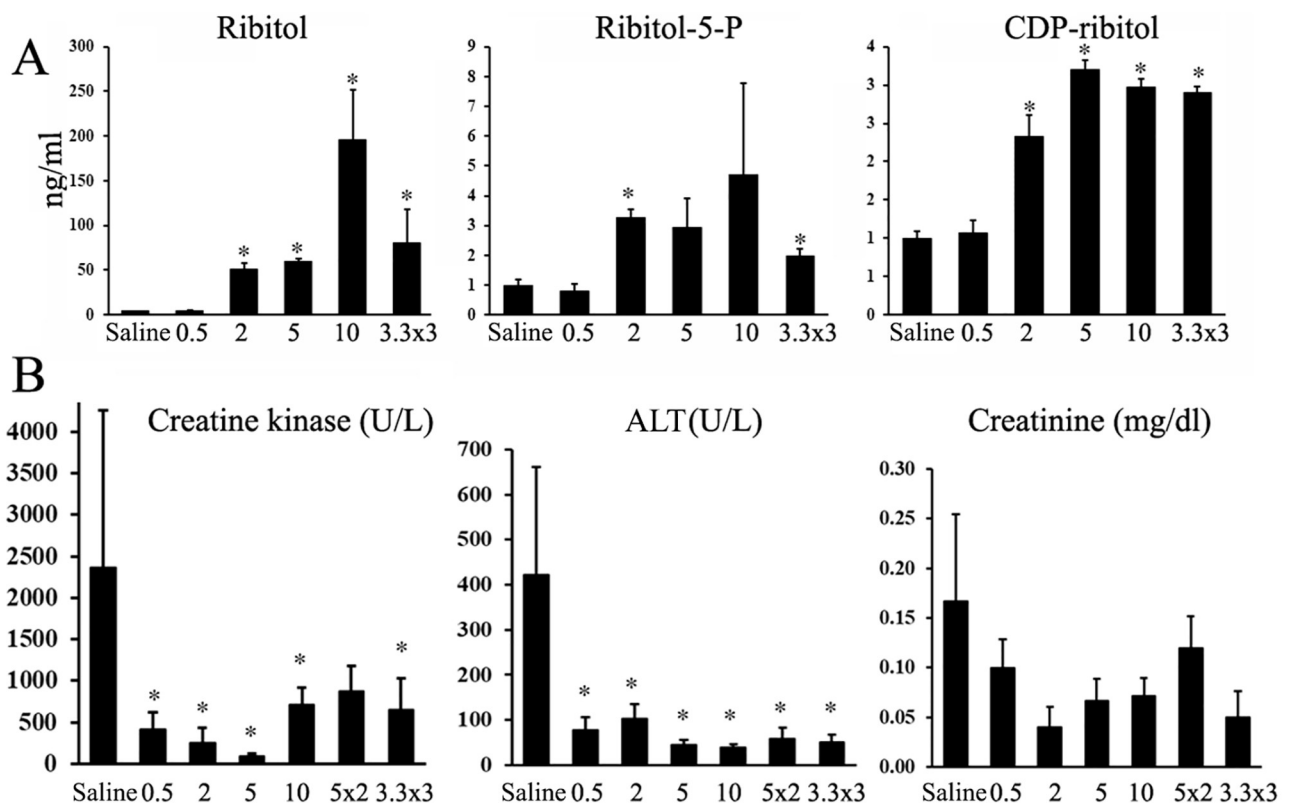


Fig 5. Detection of ribitol, ribitol-5-phosphate and CDP-ribitol and serum creatine kinase. (A) Levels of ribitol, ribitol-5-phosphate (P) and CDP-ribitol in quadriceps muscles 24 hours after last dose of ribitol treatment. Saline treatment as controls. Numbers on X axis are g/kg; x2, 2 times a day; x3, 3 times a day. (B) Ribitol treatment from 10 months of age decreases levels of serum creatine kinase and ALT. *, $p < 0.05$ $n = 3$ (A) or $n = 10$ (B).

<https://doi.org/10.1371/journal.pone.0278482.g005>

for most dose regimes except for the group with 0.5g/kg ribitol which has higher body weight than the saline control. No other side effect was recorded except that soft stool persisted and mild GI bloating was detected at the termination with daily doses of ribitol higher than 5g/kg.

Muscle function measurement showed a significant improvement in forelimb grip force for the mice treated with ribitol of 5g/kg and above although hindlimb force did not change significantly (Fig 6A and 6B). Both running distance and time with treadmill exercise were not significantly changed between treatment groups and the control except for the group treated with 10g/kg ribitol (S9A Fig in S1 File), probably due to the very later stage of the disease, which was close to the end of their life expectancy. Echocardiography showed no significant changes except that left ventricular posterior wall end diastole (LVPWd) was consistently shorter in the ribitol treated groups than the control, suggesting less hypertrophy with ribitol treatment (S9B Fig in S1 File). Similarly, no significant changes were detected in respiratory function measured by plethysmography (S10 Fig in S1 File).

Histochemical analysis of the muscles from the mice terminated 2 weeks after the last functional examination with IHH6 antibody detected a dose-dependent increase in the levels of matriglycan (S11 Fig in S1 File). This enhancement was easily identified in all the muscles examined from the mice with 5g/kg or higher ribitol groups. Consistently, H&E staining show reduced fibrosis in TA, cardiac muscle, and especially diaphragm in the groups receiving 5g/kg or higher doses of ribitol (S12 Fig in S1 File). This was further confirmed by Masson Trichrome staining as illustrated in the Fig 6C and 6D.

Life span of ribitol-treated *P448L* mice

Consistent with our previous report, all control *P448L* mutant female mice died earlier than 81 weeks with a mean survival age of 64 weeks, significantly shorter compared to their male counterpart (Fig 6E). Ribitol treatment of 0.5g/kg did not improve life span. However, treatment with daily doses of 2g/kg and above increased life span of the female mice, reaching statistical significance with the two highest dose groups of 10g/kg daily ribitol (mean survival age of 76 weeks) when compared to the control female group (Fig 6E). Life span in the male *P448L* mice treated with ribitol was similar to the saline control, most of them living longer than 80 weeks.

Discussion

Experimental therapy with the aim to restore matriglycan on α -DG for *FKRP*-related diseases by AAV-mediated gene therapy has been reported with high efficacy in preventing disease from progression in mouse models [7, 24, 25]. However, clinical trials of the therapy for the diseases with such a wide range of phenotypes are challenging and remain to be conducted. We reported earlier that, ribitol, a natural pentose alcohol delivered by drinking water *ad libitum* can restore therapeutic levels of matriglycan and ameliorate dystroglycanopathy caused by *FKRP P448L* mutation associated with severe CMD phenotype in clinic [20, 26]. In this pre-clinical evaluation, we determined the minimum effective dose of ribitol under a clinically applicable treatment regime with once and three times daily gavage. Wide-spread enhancement of matriglycan expression and some improvement in muscle functions with statistical significance were achieved with daily single dose delivery of 2g/kg body weight. Daily dose of 10g/kg showed better improvement in matriglycan expression and muscle function. However, dividing 10g/kg daily dose into 2 and 3 times for delivery appeared to have limited benefit, except that the GI side effect was clearly milder than single delivery. GI response to pentitol is likely species specific, and therefore may not be directly relevant to clinical application [27]. Nevertheless, the degree of improvement in both matriglycan expression and muscle function is similar between 5g/kg and 10g/kg groups, suggesting a possible saturation of ribitol

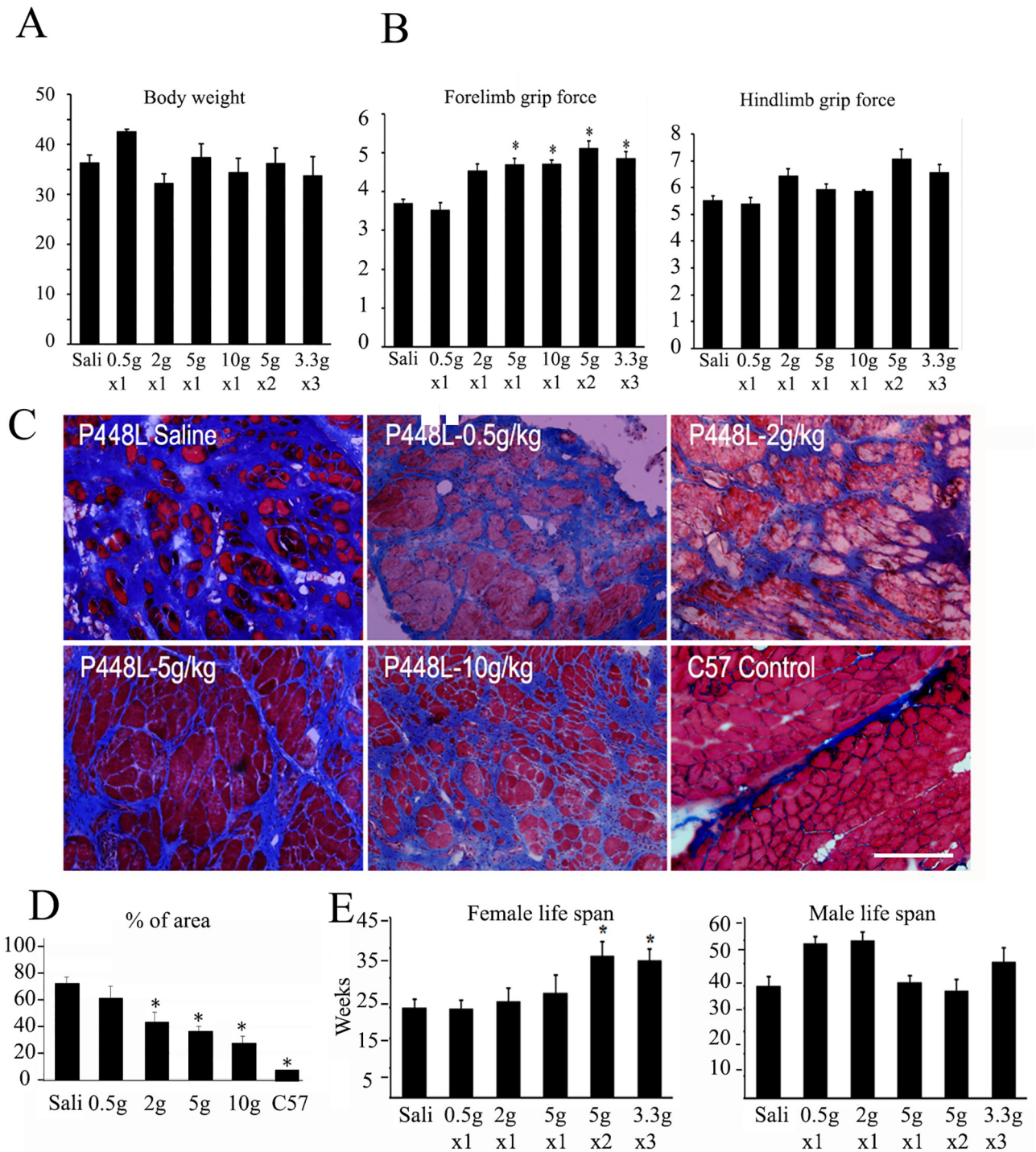


Fig 6. Effect of ribitol on body weight, muscle function, fibrosis and life span of P448L mutant mice treated with ribitol starting from 10 months of age. (A) Effect of ribitol treatment on body weight. (B) Ribitol effect on muscle function with grip force tests. (C) Masson Trichrome staining showed fibrotic area (represented by blue staining). (D) Measurement of Masson Trichrome staining of fibrotic areas. % of total area with blue staining. (E) Effect of ribitol treatment on life span of female and male mice. *, $P < 0.5$ $n = 20$ for A, B; $n = 5$ for D; $n = 10$ for E. Sali, saline treatment as control. The number of weeks is calculated starting from the treatment at 10 months of age.

<https://doi.org/10.1371/journal.pone.0278482.g006>

treatment. This is also supported by the levels of CDP-ribitol which are similar in muscle samples from groups treated with 5g/kg and 10g/kg. This, however, will unlikely limit dosing in human as the highest dose is practically difficult to achieve in clinics when the dose conversion rate from mouse to human is applied. The following factors could be important when considering dosing of ribitol in future clinical trials. First, *P448L* mutant FKRP retains possibly minimum residual function indicated by the lack of matriglycan in all muscle fibers except for a few newly regenerated revertant fibers, and by its association with CMD in clinics. The overwhelming majority of *FKRP*-related muscular dystrophy are LGMDR9 with mutations such as the common L276I mutation retaining considerably higher function as indicated by residual amounts of matriglycan and milder disease phenotypes when compared to *P448L* mutant [5, 21]. Second, our understanding that ribitol effect on matriglycan relies on residual function of FKRP in general, relative higher amount of residual matriglycan in diseased muscles might predict a higher efficiency with ribitol for inducing matriglycan. Therefore, effective dose range for treating LGMDR9 could be lower than that converted from the results of the current mouse tests. However, it should also be pointed out that different missense mutations may affect FKRP function with divergent mechanisms, from alteration in protein transportation to enzymatic activity. Thus, the degree of efficacy with ribitol treatment for different mutations could only be established by trials in a patient population.

One apparent difference between ribitol treatment and AAV gene therapy is the variation in distribution of enhanced matriglycan. Determined by differential affinity of AAV serotypes to different muscle types and selective use of promoters in different tissues, AAV gene therapy is known to produce highly variable levels of transgene expression between muscles [7, 24, 28–31]. As an example, the most widely used AAV8 and AAV9 serotypes for muscular dystrophies have shown several folds higher levels of transgene expression in cardiac muscle than in skeletal muscles. This imbalance could have long term consequence for most muscular dystrophies associated with more severe disease phenotype of skeletal muscle than that of cardiac muscle. Therefore, high doses of AAV vector for achieving effective restoration of targeted protein in skeletal muscles could lead to over-expression of the targeted protein in cardiac muscle with undesirable consequences. Vice versa, AAV doses achieving effective restoration of targeted protein in cardiac muscle may be insufficient for effective rescue of skeletal muscles. Another important weakness for AAV-mediated gene therapy is the high variation in transgene expression even within a single muscle. This has been widely reported both from preclinical animal studies and clinical trials, especially when vector doses are not sufficiently high [7, 24, 31]. Different levels of transgene expression provide different degrees of functional enhancement and variable levels of protection from contraction-related damage to fibers within a single muscle, leading to higher liability to damage, and consequently continuous degeneration and loss of transgene. In contrast, ribitol treatment provides relatively lower levels of matriglycan restoration, but with highly homogenous distribution. This can be appreciated from immunohistochemistry showing more than 90% fibers being positive in all three representative muscles (heart, diaphragm and TA) of the ribitol treated mice with all dosages, and absence of fibers with strong membrane signal above overall signal intensity. This pattern of distribution is clearly different from AAV-mediated gene therapy which produced a mixed population of fibers with no, weak, and strong expression of matriglycan within a single muscle as we reported earlier [24]. A homogenous distribution of matriglycan expression would likely provide better protection and longer-term efficacy although short-term improvement in muscle function might not be as significant as high dose AAV gene therapy. Ribitol as a pentose metabolite is likely accessible to the cells in central nervous system (CNS) which is also affected by FKRP mutations although most the patients do not show overt manifestation. It will be

interesting to determine if the same treatment could benefit the diseased CNS functionally and improve structural abnormality such as neuronal migration defect [32].

Mechanism(s) for shorter life span in untreated *P448L* mutant mice and significant increase in life span with ribitol treatment of female mice, but not male mice, are not understood. One possibility is that the shorter life-span of the female mice makes it easy for the study to demonstrate the benefit whereas such potential benefit could take much longer treatment and observation time to demonstrate in male mice. Ribitol as a natural metabolite and given relatively large amounts exogenously is expected to affect some steps of metabolic pathways as we demonstrated with the increase in R-5-P and CDP-ribitol in tissues and in serum. Understanding the mechanisms involved is important and our plan is to elucidate potential consequences of ribitol on metabolic pathways, especially the perceivable involvement in pentose phosphate pathway which is important for energy production, response to oxidative stress and building block production. It is worth noting that the levels of CDP-ribitol in the muscles appeared plateau after 5g/Kg treatment. CDP-ribitol is the final substrate for FKRP glycosyltransferase, and its level may well be critical for ribitol-induced enhancement in matriglycan. This might explain the limited further improvement by the dosage higher than 5g/Kg. Nevertheless, our current results provide sufficient preclinical efficacy and long-term safety data with suggested dosing and treatment regime for initial clinical trials.

In summary, this study demonstrates that ribitol is able to dose dependently increase matriglycan expression in clinically relevant FKRP mutant mouse model with a clinically applicable regime. Long-term ribitol treatment improves muscle pathology and function and increases life span without serious side effect. The results validate the mechanism that ribitol as a pre-substrate of FKRP glycosyltransferase is able to enhance the production of CDP-ribitol and compensate for the decreased function of mutant FKRP.

Supporting information

S1 File.
(PDF)

Acknowledgments

The authors would like to thank the Atrium Health Vivarium staffs, Leah Busbin, Kevin Todd, Marcie Allen and Attending Veterinarian Dr. Marnie S. Metzler for their support and care to the experimental animals.

Author Contributions

Conceptualization: Qi Long Lu.

Data curation: Bo Wu, Qi Long Lu.

Formal analysis: Bo Wu, Jason D. Tucker, Qi Long Lu.

Funding acquisition: Qi Long Lu.

Investigation: Bo Wu, Morgan Drains, Sapana N. Shah, Pei Juan Lu, Victoria Leroy, Jessalyn Killilee, Raegan Rawls, Anthony Blaeser.

Methodology: Bo Wu, Morgan Drains, Sapana N. Shah, Pei Juan Lu, Victoria Leroy, Raegan Rawls, Jason D. Tucker, Anthony Blaeser.

Project administration: Bo Wu, Sapana N. Shah.

Resources: Qi Long Lu.

Software: Bo Wu, Jason D. Tucker.

Supervision: Anthony Blaeser, Qi Long Lu.

Validation: Bo Wu, Morgan Drains, Pei Juan Lu, Jessalyn Killilee, Raegan Rawls, Anthony Blaeser, Qi Long Lu.

Visualization: Bo Wu, Morgan Drains, Sapana N. Shah, Pei Juan Lu, Victoria Leroy, Jessalyn Killilee, Raegan Rawls, Jason D. Tucker.

Writing – original draft: Bo Wu, Qi Long Lu.

Writing – review & editing: Jason D. Tucker, Anthony Blaeser, Qi Long Lu.

References

1. Brockington M, Blake DJ, Prandini P, Brown SC, Torelli S, Benson MA, et al. Mutations in the fukutin-related protein gene (FKRP) cause a form of congenital muscular dystrophy with secondary laminin alpha2 deficiency and abnormal glycosylation of alpha-dystroglycan. *Am J Hum Genet.* 2001; 69: 1198–1209.
2. Beltran-Valero de Bernabé D, Voit T, Longman C, Steinbrecher A, Straub V, Yuva Y, et al. Mutations in the FKRP gene can cause muscle-eye-brain disease and Walker-Warburg syndrome. *J Med Genet.* 2004; 41, e61. <https://doi.org/10.1136/jmg.2003.013870> PMID: 15121789
3. Michele DE, Barresi R, Kanagawa M, Saito F, Cohn RD, Satz JS, et al. Post-translational disruption of dystroglycan-ligand interactions in congenital muscular dystrophies. *Nature* 2002; 418: 417–422. <https://doi.org/10.1038/nature00837> PMID: 12140558
4. Brockington M, Yuva Y, Prandini P, Brown SC, Torelli S, Benson MA, et al. Mutations in the fukutin-related protein gene (FKRP) identify limb girdle muscular dystrophy 2I as a milder allelic variant of congenital muscular dystrophy MDC1C. *Hum Mol Genet.* 2001; 10: 2851–2859. <https://doi.org/10.1093/hmg/10.25.2851> PMID: 11741828
5. Brown SC, Torelli S, Brockington M, Yuva Y, Jimenez C, Feng L, et al. Abnormalities in alpha-dystroglycan expression in MDC1C and LGMD2I muscular dystrophies. *Am J Pathol.* 2004; 164: 727–737. [https://doi.org/10.1016/s0002-9440\(10\)63160-4](https://doi.org/10.1016/s0002-9440(10)63160-4) PMID: 14742276
6. Wu B, Shah SN, Lu PJ, Richardson SM, Bollinger LE, Blaeser A, et al. Glucocorticoid steroid and alendronate treatment alleviates dystrophic phenotype with enhanced functional glycosylation of alpha-dystroglycan in mouse model of Limb-Girdle Muscular Dystrophy with FKRP448L mutation. *Am J Pathol.* 2016; 186: 1635–1648.
7. Vannoy CH, Xiao W, Lu PJ, Xiao X, Lu QL. Efficacy of gene therapy is dependent on disease progression in dystrophic mice with mutations in the FKRP gene. *Mol Ther. Methods & Clinical Development* 2017; 5: 31–42. <https://doi.org/10.1016/j.omtm.2017.02.002> PMID: 28480302
8. Ervasti JM, Campbell KP. Membrane organization of the dystrophin-glycoprotein complex. *Cell* 1991; 66: 1121–1131. [https://doi.org/10.1016/0092-8674\(91\)90035-w](https://doi.org/10.1016/0092-8674(91)90035-w) PMID: 1913804
9. Ervasti JM, Campbell KP. A role for the dystrophin-glycoprotein complex as a transmembrane linker between laminin and actin. *J Cell Biol.* 1993; 122: 809–823. <https://doi.org/10.1083/jcb.122.4.809> PMID: 8349731
10. Kanagawa M, Toda T. The genetic and molecular basis of muscular dystrophy: roles of cell-matrix linkage in the pathogenesis. *J Hum Genet.* (2006; 51: 915–926. <https://doi.org/10.1007/s10038-006-0056-7> PMID: 16969582
11. Gee SH, Montanaro F, Lindenbaum MH, Carbonetto S. Dystroglycan-alpha, a dystrophin-associated glycoprotein, is a functional agrin receptor. *Cell* 1994; 77: 675–686. [https://doi.org/10.1016/0092-8674\(94\)90052-3](https://doi.org/10.1016/0092-8674(94)90052-3) PMID: 8205617
12. Talts JF, Andac Z, Göhring W, Brancaccio A, Timpl R. Binding of the G domains of laminin alpha1 and alpha2 chains and perlecan to heparin, sulfatides, alpha-dystroglycan and several extracellular matrix proteins. *EMBO J.* 1999; 18: 863–870. <https://doi.org/10.1093/emboj/18.4.863> PMID: 10022829
13. Sugita S, Saito F, Tang J, Satz JS., Campbell KP, Südhof TC. A stoichiometric complex of neuroligins and dystroglycan in brain. *J Cell Biol.* 2001; 154: 435–445.
14. Kanagawa M, Kobayashi K, Tajiri M, Many H, Kuga A, Yamaguchi Y, et al. Identification of a post-translational modification with ribitol-phosphate and its defect in muscular dystrophy. *Cell Rep.* 2016; 14: 2209–2223. <https://doi.org/10.1016/j.celrep.2016.02.017> PMID: 26923585

15. Praissman JL, Willer T, Sheikh MO, Toi A, Chitayat D, Lin YY, et al. The functional O-mannose glycan on alpha-dystroglycan contains a phospho-ribitol primed for matriglycan addition. *eLife* 2016; 5.
16. Gerin I, Ury B, Breloy I, Bouchet-Seraphin C, Bolsée J, Halbout M, et al. ISPD produces CDP-ribitol used by FKTN and FKRP to transfer ribitol phosphate onto alpha-dystroglycan. *Nat Commun.* 2016; 7: 11534.
17. Riemersma M, Froese DFS, van Tol W, Engelke UF, Kopec J, van Scherpenzeel M, et al. Human ISPD Is a cytidyltransferase required for dystroglycan O-mannosylation. *Chemistry & biology* 2015; 22: 1643–1652. <https://doi.org/10.1016/j.chembiol.2015.10.014> PMID: 26687144
18. Awano N, Blaeser A, Keramaris E, Xu L, Tucker J, Wu B, et al. Restoration of functional glycosylation of alpha-dystroglycan in FKRP mutant mice Is associated with muscle regeneration. *Am J of Pathol.* 2015; 185:2025–2037.
19. Keramaris E, Lu PL, Tucker J, Lu QL. Expression of glycosylated alpha-dystroglycan in newborn skeletal and cardiac muscles of fukutin related protein (FKRP) mutant mice. *Muscle & nerve* 2017; 55: 582–590.
20. Cataldi MP, Lu PJ, Blaeser A, Lu QL. Ribitol restores functionally glycosylated α -dystroglycan and improves muscle function in dystrophic FKRP-mutant mice. *Nat Commun.* 2018; 9: 3448.
21. Chan YM, Keramaris E, Lidov HG, Norton JH, Zinchenko N, Gruber HE, et al. Fukutin-related protein is essential for mouse muscle, brain and eye development and mutation recapitulates the wide clinical spectrums of dystroglycanopathies. *Hum Mol Genet.* 2010; 19: 3995–4006. <https://doi.org/10.1093/hmg/ddq314> PMID: 20675713
22. Blaeser A, Keramaris E, Chan YM, Sparks S, Cowley D, Xiao X, et al. Mouse models of fukutin-related protein mutations show a wide range of disease phenotypes. *Hum Genet.* 2013; 132: 923–934. <https://doi.org/10.1007/s00439-013-1302-7> PMID: 23591631
23. Blaeser A, Awano H, Wu B, Lu QL. Progressive dystrophic pathology in diaphragm and impairment of cardiac function in FKRP P448L mutant mice. *PLoS ONE* 2016; 11(10): e0164187.
24. Vannoy CH, Leroy V, Lu QL. Dose-dependent effects of FKRP gene-replacement therapy on functional rescue and longevity in dystrophic mice. *Mol Ther Methods Clin Dev.* 2018; 11: 106–120. <https://doi.org/10.1016/j.omtm.2018.10.004> PMID: 30417025
25. Tucker JD, Lu PJ, Xiao X, Lu QL. Overexpression of mutant FKRP restores functional glycosylation and improves dystrophic phenotype in FKRP mutant mice. *Mol Ther Nucleic Acids.* 2018; 11:216–227. <https://doi.org/10.1016/j.omtm.2018.02.008> PMID: 29858056
26. Cataldi MP, Blaeser A, Lu PJ, Leroy V, Lu QL. ISPD overexpression enhances ribitol-induced glycosylation of α -dystroglycan in dystrophic FKRP mutant mice. *Mol Ther Methods Clin Dev.* 2020; 17: 271–280.
27. Schmid RD, Hovda LR. Acute hepatic failure in a dog after xylitol ingestion. *J Med Toxicol.* 2016; 12(2): 201–205. <https://doi.org/10.1007/s13181-015-0531-7> PMID: 26691320
28. Hakim CH, Yue Y, Shin JH, Williams RR, Zhang K, F Smith BF, et al. Systemic gene transfer reveals distinctive muscle transduction profile of tyrosine mutant AAV-1, -6, and -9 in neonatal dogs. *Mol Ther Methods Clin Dev.* 2014; 1:14002 <https://doi.org/10.1038/mtm.2014.2> PMID: 25105153
29. Hinderer C, Katz N, Buza EL, Dyer C, Goode T, Bell P, et al. Severe Toxicity in nonhuman primates and piglets following high-dose intravenous administration of an adeno-associated virus vector expressing human SMN. *Hum Gene Ther.* 2018; 29(3): 285–298. <https://doi.org/10.1089/hum.2018.015> PMID: 29378426
30. Crudele JM, Chamberlain JS. AAV-based gene therapies for the muscular dystrophies. *Hum Mol Genet.* 2019; 28(R1):R102–R107 <https://doi.org/10.1093/hmg/ddz128> PMID: 31238336
31. Hakim CH, Clément H, Wasala LP, Yang HT, Yue Y, Zhang K, et al. Micro-dystrophin AAV Vectors made by transient transfection and herpesvirus system are equally potent in treating mdx mouse muscle disease. *Mol Ther Methods Clin Dev.* 2020; 18:664–678 <https://doi.org/10.1016/j.omtm.2020.07.004> PMID: 32775499
32. Palmieri A, Manara R, Bello L, Mento G, Lazzarini L, Borsato C, et al. Cognitive profile and MRI findings in limb-girdle muscular dystrophy 2I. *J Neurol* 2011; 258(7):1312–20 <https://doi.org/10.1007/s00415-011-5930-3> PMID: 21293871